INTERNATIONAL SCIENTIFIC JOURNAL OF ENGINEERING AND MANAGEMENT ISSN: 2583-6129
VOLUME: 03 ISSUE: 04 | APRIL – 2024 DOI: 10.55041/ISJEM01462
AN INTERNATIONAL SCHOLARLY || MULTIDISCIPLINARY || OPEN ACCESS || INDEXING IN ALL MAJOR DATABASE & METADATA

II.

A COMPUTATIONAL FLUID DYNAMICS STUDY ON FLOW PATTERNS IN A SOLAR AIR HEATER WITH ARTIFICIAL ROUGHNESS

[1]Anshu Kumar Tiwari, [2]Inder Singh Nagar
M.Tech Scholor[1], Assistant Professor[2]
[1,2]Department of Mechanical Engineering
[1,2]School of Research And Technology, People's University, Bhopal (M.P.)

Abstract— ***Solar air heaters, renowned for their simplicity in design, offer an economical solution and stand as the most prevalent solar energy collection devices. However, their thermal efficiency is notably diminished due to the relatively low convective heat transfer coefficient between the absorber plate and the air, resulting in elevated absorber plate temperatures and substantial heat loss to the surroundings. This study delves into the intricacies of heat transfer within a solar air heater utilizing Computational Fluid Dynamics (CFD). Specifically, it examines the impact of Reynolds number variation on Nusselt number. The investigation employs ANSYS FLUENT 16, a commercial finite volume package, to analyze and visually depict the flow characteristics within the duct of the solar air heater.***

Index Terms— Solar Air Heater, Heat transfer, Pressure Drop, CFD.

I. INTRODUCTION

The solar air heater stands as a fundamental apparatus for the conversion of solar energy into thermal energy. Due to its straightforward design, solar air heaters emerge as economical and extensively utilized solar energy collectors. Primarily employed for space heating, timber seasoning, and industrial product curing, these heaters also demonstrate effectiveness in the drying and curing processes of concrete and clay building components. Typically comprising an absorber plate, rear plate, insulation beneath the rear plate, a transparent cover on the exposed side, and airflow occurring between the absorber and rear plates, conventional solar air heaters boast simplicity in design and demand minimal maintenance.

Nonetheless, their efficiency is hindered by a low heat transfer coefficient between the absorber plate and air, often necessitating surface roughening within the airflow passage to alleviate this limitation.

The utilization of artificial roughness initially emerged from Joule's pioneering work [1], aimed at amplifying heat transfer coefficients during steam condensation within tubes. Since then, numerous experimental inquiries have delved into the application of artificial roughness across various domains, including gas turbine cooling, electronics cooling, nuclear reactors, and compact heat exchangers. Nunner [2] stands out as the pioneer in formulating a flow model, drawing parallels

between this model and the temperature distribution observed in smooth tube flow, particularly under elevated Prandtl numbers.

According to the proposed flow model, roughness plays a role in diminishing the thermal resistance within the turbulence-dominated wall region while minimally impacting the viscous region. This assertion finds quantification through the Prandtl analogy, where Pr is substituted by (f/fs)Pr. As per this model, it is predicted that the ratio of Stanton number to its smooth tube counterpart (St/Sts) diminishes with increasing Prandtl numbers. Furthermore, the proposed flow model posits that St/Sts remains unaffected by the nature of the roughness. A friction correlation tailored for flow over sand-grain roughness was subsequently developed.

I.

Prasad and Mullick [5] were pioneers in utilizing artificial roughness, such as small diameter wires attached to the underside of absorber plates, to enhance the thermal performance of solar air heaters for drying purposes. After their work, numerous experimental investigations have been conducted on solar air heaters involving roughness elements of varying shapes, sizes, and orientations to optimize roughness geometry [6-7].

Chaube et al. [8] performed a Computational Fluid Dynamics (CFD) analysis on the heat transfer and fluid flow characteristics of an artificially roughened solar air heater. Similarly, Kumar and Saini [9] conducted a CFD analysis on fluid flow and heat transfer characteristics of solar air heaters with arc-shaped artificial roughness on absorber plates. Karmare and Tikekar [10] conducted a CFD investigation on fluid flow and heat transfer in a solar air heater duct using metal grit ribs as roughness elements on the absorber plate. Yadav and Bhagoria [11] focused on numerical prediction to study only the heat transfer behavior of rectangular ducts of solar air heaters with triangular rib roughness on the absorber plate. Additionally, they presented numerical predictions of fluid flow and heat transfer in conventional solar air heaters through CFD [12], utilizing the ANSYS FLUENT 12.1 software.
Furthermore, Yadav and Bhagoria [13-14] provided an extensive literature survey on various CFD investigations on artificially roughened solar air heaters. Various types of turbulator elements have been widely employed to enhance heat transfer characteristics [15-69].
The objective of our study is to enhance the prediction of flow in solar air heaters. We aim to implement a near-wall function for Turbulent Kinetic Energy (TKE) in the Computational Fluid Dynamics code Fluent. Second-order upwind and the SIMPLE algorithm were utilized to discretize the governing equations. The FLUENT software is employed to solve the mathematical equations governing fluid flow, heat transfer, and related phenomena for a given physical problem.

II. CFD MODELING AND ANALYSIS

Computational Fluid Dynamics (CFD) encompasses the computational analysis aimed at solving the governing equations of fluid flow numerically, thereby progressing the solution spatially or temporally to derive a numerical depiction of the desired flow field. These equations can accommodate various conditions, including steady or unsteady flow, compressible or incompressible flow, and both inviscid and viscous flows, while also incorporating non-ideal and reactive fluid behaviors. The choice of equation form is contingent upon the specific application at hand. Advancements in this field are marked by the intricate nature of geometric configurations, the underlying flow physics, and the computational resources required to attain a solution.
The CFD analysis presented utilizes a 2-dimensional computational domain illustrated in Figure 1, with dimensions of height (H) at 20 mm and width (W) at 100 mm. For the current investigation, a 2-dimensional computational domain resembling the roughened solar air heater domain employed by Yadav and Bhagoria [14] has been adopted.

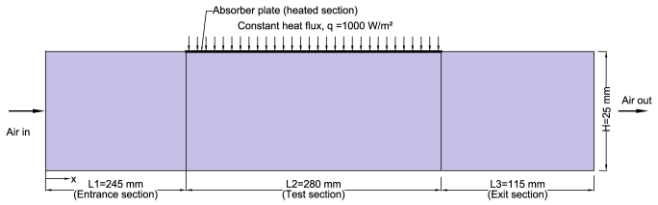

Fig. 1. 2-D computational domain

After defining the computational domain, a non-uniform mesh is generated to optimize resolution. The mesh prioritizes higher cell density near the plate to effectively capture the turbulent boundary layer, which is significantly thinner compared to the overall flow field height. Boundary conditions are then specified following mesh generation. The left and right edges are designated as the duct inlet and outlet respectively, while the top edge represents the surface and the bottom edges correspond to the inlet length, outlet length, and solar plate. All internal edges of the 2D duct are defined as turbulator walls.

The meshing process utilizes ANSYS ICEM CFD V16 software, with a focus on creating very fine grids to accommodate low-Reynolds-number turbulence models. The resultant non-uniform quadrilateral mesh comprises 161,568 quad cells with a cell size of 0.22 mm, deemed appropriate for resolving the laminar sub-layer. To ensure grid independence, a series of tests are conducted where the cell count varies from 103,231 to 197,977 in five increments. It is observed that beyond 161,568 cells, further increases have less than 1% impact on both Nusselt number and friction factor values, which serve as criteria for grid independence.

In selecting the turbulence model, previous experimental data is simulated using various low Reynolds number models such as the Standard k-ω model, Renormalization-group kε model, Realizable kε model, and Shear stress transport k-ω model. Results from these models are compared against experimental data, with the RNG k-ε model exhibiting the closest agreement. The working fluid, assumed to be air, is treated as incompressible given its negligible variation within the duct's operating range. The mean inlet velocity is determined via the Reynolds number, and velocity boundary conditions are applied at the inlet while outflow conditions are set at the outlet.

Governing equations for fluid flow, heat transfer, and related phenomena are solved using the FLUENT software, with discretization performed using second-order upwind and the SIMPLE algorithm. These equations encapsulate the behavior of the fluid flow system under study, providing insights into heat transfer and other pertinent phenomena within the specified physical problem.

III. RESULTS AND DISCUSSIONS

The findings are illustrated through graphical representations, depicting the average Nusselt number across various Reynolds numbers. Additionally, temperature and velocity contours are depicted at specific sections for a fixed Reynolds number. In Figure 2, the influence of Reynolds number on the average Nusselt number is displayed for different values of relative roughness height (e/D), with a fixed pitch.

It's observed that as the Reynolds number increases, there's a corresponding rise in the average Nusselt number. This trend is attributed to the heightened turbulence intensity resulting from increased turbulence kinetic energy and turbulence dissipation rate.

Among the tested configurations, the duct with a relative roughness height of 0.06 exhibits the highest Nusselt number at a Reynolds number of 18000. Conversely, the duct with a relative roughness height (e/D) of 0.015 demonstrates the lowest Nusselt number at a Reynolds number of 3800. Notably, the maximum enhancement in the average Nusselt number is determined to be 2.78 times that of a smooth duct, observed for a relative roughness height of 0.06.

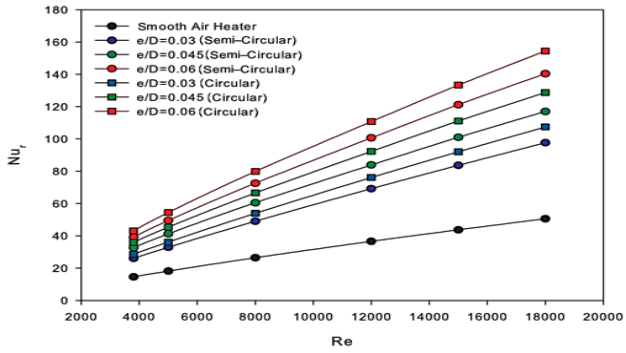

Fig. 2. Variation in Nusselt number

The heat transfer process is effectively visualized and elucidated through the contour plot depicting turbulence intensity. Turbulence levels decrease in proximity to the rib and wall within the flow field, while a zone of heightened turbulence intensity emerges between adjacent ribs near the primary flow path. This underscores the significant impact of turbulence intensity on augmenting heat transfer.

As depicted in Fig 3, the friction factor consistently diminishes as Reynolds numbers increase across all scenarios, aligning with expectations due to the suppression of the laminar sub-layer in fully developed turbulent flow within the duct. Notably, the highest and lowest points of the friction factor occur at relative roughness heights (e/d) of 0.06 and 0.015,

respectively, within the range of parameters examined. Furthermore, it's evident that the maximum average friction factor enhancement reaches 4.24 times that of a smooth duct at a relative roughness height of 0.06 and a Reynolds number of 3800.

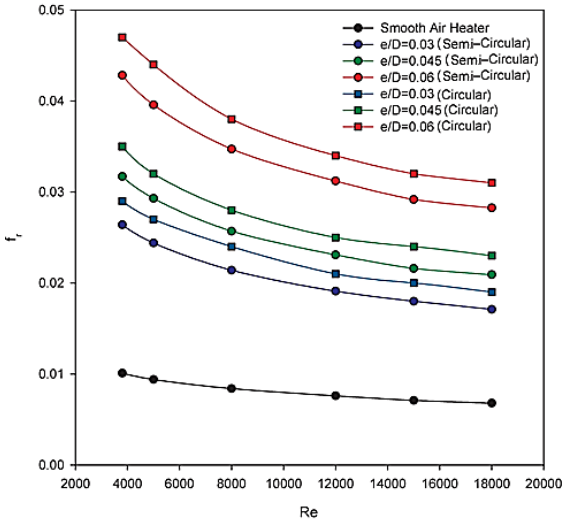

Fig. 3. Variation in Friction factor

The fluid friction phenomenon becomes apparent through the pressure distribution around circular ribs, as depicted in Figure 4. This pressure contour plot exhibits a distinct pattern. A comparable pattern emerges when examining the pressure distribution around semi-circular ribs. The flow friction characteristics are elucidated through the analysis of pressure contours surrounding semi-circular ribs.

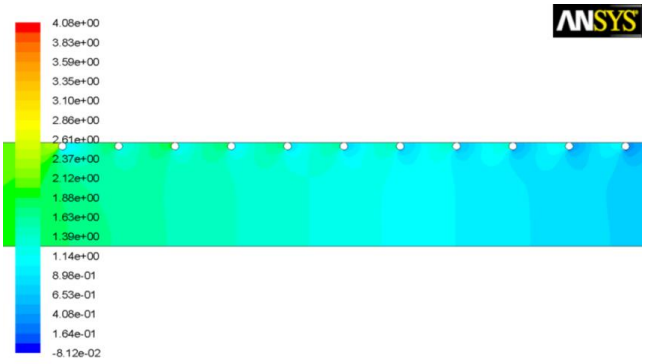

Fig. 4. Contour plot

To authenticate the current numerical model, it underwent a validation process by juxtaposing its outcomes with existing experimental data. The review of literature concerning artificially roughened solar air heater systems indicates a typical range for the relative roughness height between 0.03 and 0.047. Comparing the optimal relative roughness height from the current computational fluid dynamics (CFD) simulation with established experimental or widely acknowledged numerical findings, it's evident that the CFD model's optimum value stands at 0.045 for ribs shaped in circular and semi-circular sections. This value falls within the acknowledged range of 0.033 to 0.043. Consequently, a notable concordance is observed between the CFD outcomes and the experimental/numerical results.

IV. CONCLUSION

The impact of relative roughness pitch and Reynolds number on the heat transfer coefficient and friction factor was investigated. Computational Fluid Dynamics (CFD) analysis was conducted within a medium Reynolds number flow range (Re = 3800–18,000) in a rectangular duct featuring protrusions as roughness elements on one broad wall under uniform heat flux conditions. The findings are summarized as follows:

1. The average Nusselt number demonstrates an increase with a rising Reynolds number. The peak average Nusselt number occurs at a relative roughness height of 0.06, particularly evident at a higher Reynolds number of 18,000.
2. Conversely, the average friction factor shows a decrease as the Reynolds number increases. The highest average friction factor is observed at a relative roughness height of 0.06, notably at a lower Reynolds number of 3800.
3. The Renormalization-group (RNG) k-ε turbulence model exhibits close alignment with experimental findings, instilling confidence in the CFD predictions made in this study. Validation of the RNG k-ε turbulence model was performed for a smooth duct, and a grid independence test was executed to assess its consistency with an increasing number of cells.

4. Comparing available experimental data with computational results reveals a discrepancy of less than ±10%. Thus, it can be inferred that the computational outcomes obtained in this study are reasonably accurate.

REFERENCES

[1] Joule JP. On the surface condensation of steam. Philosophical Transactions of the Royal Society of London 1861; 151: 133-160.
[2] Nunner W. Heat transfer and pressure drop in rough pipes. VDI-Forsch 1956; 22: 445-B, English trans, AERE Lib./Trans 1958; 786.
[3] Nikuradse J. Laws of flow in rough pipes. NACA Technical Memorandum 1950; 1292.
[4] Dippery DF, Sabersky RH. Heat and momentum transfer in smooth and rough tubes at various Prandtl number. Int J Heat Mass Transfer 1963; 6: 329–53.
[5] Prasad K, Mullick SC. Heat transfer characteristics of a solar air heater used for drying purposes. Appl Energy 1983; 13(2): 83-93.
[6] Hans VS, Saini RP, Saini JS. Performance of artificially roughened solar air heaters- A review. Renewable and Sustainable Energy Reviews 2009; 13: 1854–1869.
[7] Bhushan B, Singh R. A review on methodology of artificial roughness used in duct of solar air heaters. Energy 2010; 35: 202–212.
[8] A. Chaube, P.K. Sahoo, S.C. Solanki, Analysis of heat transfer augmentation and flow characteristics due to rib roughness over absorber plate of a solar air heater, Renewable Energy 31 (2006) 317-31.
[9] S. Kumar, R.P. Saini, CFD based performance analysis of a solar air heater duct provided with artificial roughness, Renewable Energy 34 (2009) 1285-91.
[10] S.V. Karmare, A.N. Tikekar, Analysis of fluid flow and heat transfer in a rib grit roughened surface solar air heater using CFD, Solar Energy 84 (2010) 409–17.
[11] A.S. Yadav, J.L. Bhagoria, A CFD analysis of a solar air heater having triangular rib roughness on the absorber plate, International Journal of ChemTech Research 5(2) (2013) 964-71.
[12] A.S. Yadav, J.L. Bhagoria, A CFD based heat transfer and fluid flow analysis of a conventional solar air heater, Journal of Engineering Science and Management Education 6(2) (2013) 137-146.
[13] A.S. Yadav, J.L. Bhagoria, Heat transfer and fluid flow analysis of solar air heater: a review of CFD approach, Renewable and Sustainable Energy Reviews 23 (2013) 60-79.
[14] A.S. Yadav, J.L. Bhagoria. A CFD based heat transfer and fluid flow analysis of a solar air heater provided with circular transverse wire rib roughness on the absorber plate, Energy, Elsevier, 55 (2013) 1127-1142. Team. Philosophical Transactions of the Royal Society of London 1861; 151: 133-160.
[15] Hans VS, Saini RP, Saini JS. Performance of artificially roughened solar air heaters- A review. Renewable and Sustainable Energy Reviews 2009; 13: 1854–1869.
[16] Bhushan B, Singh R. A review on methodology of artificial roughness used in duct of solar air heaters. Energy 2010; 35: 202–212.
[17] Yadav, A. S., and Thapak, M. K. "Artificially roughened solar air heater: A comparative study," International Journal of Green Energy vol. 13, no. 2, 2016, pp. 143-172.
[18] Yadav Anil Singh, Thapak MK. Artificially roughened solar air heater: experimental investigations. Renewable and Sustainable Energy Reviews 2014; 36: 370-411.
[19] Yadav AS, Bhagoria JL. A CFD based performance analysis of an artificially roughened solar air heater having equilateral triangular sectioned rib roughness on the absorber plate. International Journal of Heat and Mass Transfer 2014; 70: 1016–1039.
[20] Yadav AS, Bhagoria JL. Heat transfer and fluid flow analysis of solar air heater: a review of CFD approach. Renewable and Sustainable Energy Reviews 2013; 23: 60-79.
[21] Yadav AS, Bhagoria JL. A CFD based heat transfer and fluid flow analysis of a solar air heater provided with circular transverse wire rib roughness on the absorber plate. Energy 2013; 55: 1127-42.
[22] Yadav AS, Bhagoria JL. Modeling and simulation of turbulent flows through a solar air heater having square sectioned transverse rib roughness on the absorber plate. The Scientific World Journal 2013. DOI: 10.1155/2013/827131.
[23] Yadav AS, Bhagoria JL. A numerical investigation of turbulent flows through an

artificially roughened solar air heater. Numerical Heat Transfer A 2014; 65: 679–698.

[24] Yadav AS, Bhagoria JL. Numerical investigation of flow through an artificially roughened solar air heater. International Journal of Ambient Energy 2013. DOI: 10.1080/01430750.2013.823107 (Article in press).

[25] Yadav AS, Bhagoria JL. Heat transfer and fluid flow analysis of an artificially roughened solar air heater: a CFD based investigation. Frontiers in Energy 2014; 8(2): 201-211.

[26] Yadav AS, Bhagoria JL. A CFD analysis of a solar air heater having triangular rib roughness on the absorber plate. International Journal of ChemTech Research 2013; 5(2): 964-71.

[27] Yadav AS, Bhagoria JL. A CFD based heat transfer and fluid flow analysis of a conventional solar air heater. Journal of Engineering Science and Management Education 2013; 6(2): 137-46.

[28] Yadav AS, Bhagoria JL. A numerical investigation of square sectioned transverse rib roughened solar air heater. International Journal of Thermal Sciences 2014; 79: 111-131.

[29] Ahn S. W. 2001. The effects of roughness types on friction factors and heat transfer in roughened rectangular duct. Int. J. Heat and Mass transfer. 28, 933-942.

[30] Chandra P.R., Alexander C.R, Han J.C. 2003. Heat transfer and friction behaviors in rectangular channels with varying number of ribbed walls. Int. J. Heat and Mass transfer. 46, 481–495.

[31] Tanda Giovanni. 2004. Heat transfer in rectangular channels with transverse and V-shaped broken ribs. Int. J. Heat and Mass transfer. 47, 229–243.

[32] Tariq Andallib, Singh Kamlesh and Panigrahi P.K. 2002. Detailed measurement of heat transfer and flow characteristics in rectangular duct with rib turbulators mounted on the bottom surface. Engineering Turbulence Modelling and Experiments. 5, 445 - 454.

[33] Won S.Y., Ligrani P.M. 2004. Comparisons of flow structure and local Nusselt numbers in channels with parallel- and crossed-rib turbulators. 47, 1573–1586.

[34] Wang Lieke, Sunden Bengt. 2004.An experimental investigation of heat transfer and fluid flow in a rectangular duct with broken v-shaped ribs. Experimental Heat Transfer. 17,243–259.

[35] Liu Ye-Di, Diaz L. A., Suryanarayana N. V. 1984. Heat transfer enhancement in air heating fiat-plate solar collectors. Trans. ASME, J. of Solar Energy Engg.106, 358-363.

[36] Yadav, A. S. "Augmentation of heat transfer in double pipe heat exchanger using full & half-length twisted tape inserts," CSVTU Research Journal vol. 1, no. 1, 2008, pp. 67-73.

[37] Yadav, A. S. "Experimental investigation of heat transfer performance of double pipe U-bend heat exchanger using full length twisted tape," International Journal of Applied Engineering Research vol. 3, no. 3, 2008, pp. 399-407.

[38] Yadav, A. S. "Effect of half-length twisted-tape turbulators on heat transfer and pressure drop characteristics inside a double pipe u-bend heat exchanger," Jordan Journal of Mechanical and Industrial Engineering vol. 3, no. 1, 2009, pp. 17-22.

[39] Yadav, A. S., and Bhagoria, J. L. "An Economic Analysis of a Solar System," Corona Journal of Science and Technology vol. 2, no. 1, 2013, pp. 3-7.

[40] Yadav, A. S., and Bhagoria, J. L. "Renewable Energy Sources-An Application Guide: Energy for Future," International Journal of Energy Science vol. 3, no. 2, 2013, pp. 70-90.

[41] Bhaskar, B., Bhadoria, R. S., and Yadav, A. S. "Transportation system of coal distribution: a fuzzy logic approach using MATLAB," Corona Journal of Science and Technology vol. 2, no. 3, 2013, pp. 20-30.

